Stereotactic recording and stimulation procedures. Standard methods were used for functional stereotactic procedures[29]. Microelectrode recordings and stimulation were performed with either glass- or parylene-coated tungsten microelectrodes. Our initial target was chosen near the ventral border (at or close to the line between the anterior and posterior commissures of the ventrocaudal nucleus, in a sagittal plane 14–15 mm lateral to the midline. Subsequent electrode trajectories were appropriate for the patient's site of pain. Each electrode trajectory was made through the thalamus in a parasagittal plane. The standard search procedure during each penetration consisted of recording the neuronal activity continuously as the electrode was advanced. At sites of spontaneous neuronal activity, stimuli were applied to the joints (passive and/or active movements), muscles (squeeze) and skin (brush and hot and cold probes) to delineate receptive fields. At intervals of 0.5–1 mm, the microelectrode was used to deliver brief trains of electrical stimuli (1 s, 300-Hz trains of 0.2 ms monophasic (tip negative) pulses of up to 100 μA) to determine the threshold for sensation, and the patient was asked to describe the location (projected field) and quality of any evoked sensation. To assess abnormalities in body representations in each amputee, the length along each trajectory that represented the stump region was summed and expressed as a percentage of the total sampled length of tactile ventrocaudal nucleus in that patient. The data obtained from non-amputee patients with movement disorders was sampled from a comparable region of the ventrocaudal nucleus[22].

Received 15 July; accepted 25 October 1997.

1. Sherman, R. A., Sherman, C. J. & Parker, L. Chronic phantom and stump pain among American veterans: results of a survey. *Pain* **18**, 83–95 (1984).
2. Carlen, P. L., Wall, P. D., Nadvorna, H. & Steinbach, T. Phantom limbs and related phenomena in recent traumatic amputations. *Neuroloby* **28**, 211–217 (1978).
3. Melzack, R. Phantom limbs and the concept of a neuromatrix. *Trends Neurosci.* **13**, 88–92 (1990).
4. Calford, M. B. & Tweedale, R. Immediate expansion of receptive fields of neurons in area 3b of macaque monkeys after digit denervation. *Somatosens. Mot. Res.* **8**, 249–260 (1991).
5. Wall, J. T., Huerta, M. F. & Kaas, J. H. Changes in the cortical map of the hand following postnatal median nerve injury in monkeys: Modification of somatotopic aggregates. *J. Neurosci.* **12**, 3445–3455 (1992).
6. Rasmusson, D. D. Reorganization of raccoon somatosensory cortex following removal of the fifth digit. *J. Comp. Neurol.* **205**, 313–326 (1982).
7. Flor, H. *et al.* Phantom-limb pain as a perceptual correlate of cortical reorganization following arm amputation. *Nature* **375**, 482–484 (1995).
8. Elbert, T. *et al.* Extensive reorganization of the somatosensory cortex in adult humans after nervous system injury. *Neuroreport* **5**, 2593–2597 (1994).
9. Yang, T. T. *et al.* Noninvasive detection of cerebral plasticity in adult human somatosensory cortex. *Neuroreport* **5**, 701–704 (1994).
10. Kew, J. J. M. *et al.* Abnormal access of axial vibrotactile input to deafferented somatosensory cortex in human upper limb amputees. *J. Neurophysiol.* **77**, 2753–2764 (1997).
11. Merzenich, M. M. *et al.* Topographic reorganization of somatosensory cortical areas 3B and 1 in adult monkeys following restricted deafferentation. *Neuroscience* **8**, 33–55 (1983).
12. Pons, T. P. *et al.* Massive cortical reorganization after sensory deafferentation in adult macaques. *Science* **252**, 1857–1860 (1991).
13. Florence, S. L. & Kaas, J. H. Large-scale reorganization at multiple levels of the somatosensory pathway follows therapeutic amputation of the hand in monkeys. *J. Neurosci.* **15**, 8083–8095 (1995).
14. Merzenich, M. M. *et al.* Somatosensory cortical map changes following digit amputation in adult monkeys. *J. Comp. Neurol.* **224**, 591–605 (1984).
15. Rasmusson, D. Changes in the organization of the ventroposterior lateral thalamic nucleus after digit removal in adult raccoon. *J. Comp. Neurol.* **364**, 92–103 (1996).
16. Wall, P. D. & Egger, M. D. Formation of new connexions in adult rat brains after partial deafferentation. *Nature* **232**, 542–545 (1971).
17. Tasker, R. R. & Kiss, Z. H. T. The role of the thalamus in functional neurosurgery. *Neurosurg. Clin. N. Am.* **6**, 73–104 (1995).
18. Tsoukatos, J., Davis, K. D., Tasker, R. R., Lozano, A. M. & Dostrovsky, J. O. Deafferentation and local damage give rise to bursting activity in thalamus of awake patients. *Soc. Neurosci. Abstr.* **22**, 98 (1996).
19. Lenz, F. A. *et al.* Single-unit analysis of the human ventral thalamic nuclear group: Somatosensory responses. *J. Neurophysiol.* **59**, 299–316 (1988).
20. Davis, K. D., Kiss, Z. H. T., Tasker, R. R. & Dostrovsky, J. O. Thalamic stimulation-evoked sensations in chronic pain patients and in nonpain (movement disorder) patients. *J. Neurophysiol.* **75**, 1026–1037 (1996).
21. Lenz, F. A. *et al.* Characteristics of somatotopic organization and spontaneous neuronal activity in the region of the thalamic principal sensory nucleus in patients with spinal cord transection. *J. Neurophysiol.* **72**, 1570–1587 (1994).
22. Kiss, Z. H. T., Dostrovsky, J. O. & Tasker, R. R. Plasticity in human somatosensory thalamus as a result of deafferentation. *Stereotact. Funct. Neurosurg.* **62**, 153–163 (1994).
23. Halligan, P. W., Marshall, J. C., Wade, D. T., Davey, J. & Morrison, D. Thumb in cheek? Sensory reorganization and perceptual plasticity after limb amputation. *Neuroreport* **4**, 233–236 (1993).
24. Aglioti, S., Cortese, F. & Franchini, C. Rapid sensory remapping in the adult human brain as inferred from phantom breast perception. *Neuroreport* **5**, 473–476 (1994).
25. Knecht, S. *et al.* Cortical reorganization in human amputees and mislocalization of painful stimuli to the phantom limb. *Neurosci. Lett.* **201**, 262–264 (1995).
26. Clarke, S., Regli, L., Janzer, R. C., Assal, G. & De Tribolet, N. Phantom face: Conscious correlate of neural reorganization after removal of primary sensory neurones. *Neuroreport* **7**, 2853–2857 (1996).
27. Doetsch, G. S. Progressive changes in cutaneous trigger zones for sensation referred to a phantom hand: a case report and review with implications for cortical reorganization. *Somatosens. Mot. Res.* **14**, 6–16 (1997).
28. Ramachandran, V. S. Behavioral and magnetoencephalographic correlates of plasticity in the adult human brain. *Proc. Natl Acad. Sci. USA* **90**, 10413–10420 (1993).
29. Lenz, F. A. *et al.* Methods for microstimulation and recording of single neurons and evoked potentials in the human central nervous system. *J. Neurosurg.* **68**, 630–634 (1988).

Acknowledgements. We thank F. Lenz for assistance with data collection from two of the patients; M. Teofilo for technical assistance with computer reconstructions of patient data; and A. D. Craig and J. Katz for comments on an earlier draft of this manuscript. This work was supported by the Medical Research Council of Canada and NIH.

Correspondence and requests for materials should be addressed to K.D.D. (e-mail: kdavis@playfair.utoronto.ca).

Deficiency of presenilin-1 inhibits the normal cleavage of amyloid precursor protein

Bart De Strooper*†, Paul Saftig†‡, Katleen Craessaerts*, Hugo Vanderstichele§, Gundula Bühde‡, Wim Annaert*, Kurt Von Figura‡ & Fred Van Leuven*

** Experimental Genetics Group, Flemish Institute for Biotechnology (VIB4), Center for Human Genetics, K.U.Leuven, Belgium*
§ Innogenetics NV, Industriepark Zw.7, 9057 Gent, Belgium
‡ Zentrum Biochemie und Molekular Zellbiologie, Abteilung Biochemie II, Universität Göttingen, 37073 Göttingen, Germany
† These authors contributed equally to this work.

Point mutations in the presenilin-1 gene (*PS1*) are a major cause of familial Alzheimer's disease. They result in a selective increase in the production of the amyloidogenic peptide amyloid-β(1–42) by proteolytic processing of the amyloid precursor protein (APP)[1–4]. Here we investigate whether PS1 is also involved in normal APP processing in neuronal cultures derived from PS1-deficient mouse embryos. Cleavage by α- and β-secretase[5] of the extracellular domain of APP was not affected by the absence of PS1, whereas cleavage by γ-secretase of the transmembrane domain of APP was prevented, causing carboxyl-terminal fragments of APP to accumulate and a fivefold drop in the production of amyloid peptide. Pulse-chase experiments indicated that PS1 deficiency specifically decreased the turnover of the membrane-associated fragments of APP. As in the regulation of cholesterol metabolism by proteolysis of a membrane-bound transcription factor[6], PS1 appears to facilitate a proteolytic activity that cleaves the integral membrane domain of APP. Our results indicate that mutations in *PS1* that manifest clinically cause a gain of function and that inhibition of PS1 activity is a potential target for anti-amyloidogenic therapy in Alzheimer's disease.

Mice deficient in the expression of PS1 ($PS1^{-/-}$ mice) were generated by homologous recombination (see Methods). We confirmed that homozygous $PS1^{-/-}$ mice die late in embryogenesis[7,8]. Growth of the embryo was severely retarded, being most evident in the caudal region as a stubby tail. It has been proposed that this phenotype is a result of disturbed Notch signalling[7,8]. The embryonic lethality of $PS1^{-/-}$ mice precludes further analysis of the possible effects on APP metabolism in living animals. Therefore, brain cultures were generated from living $PS1^{-/-}$ embryos at day 14 post coitum (pc) according to protocols used previously for hippocampal neurons[9–12]. Cell yields were $7.6(\pm 1.6) \times 10^6$ cells for $PS1^{+/+}$ ($n = 6$), $7.8(\pm 1.3) \times 10^6$ cells for $PS1^{+/-}$ ($n = 7$), and $6.0(\pm 1.3) \times 10^6$ cells for $PS1^{-/-}$ embryos ($n = 3$). Cultures derived from littermate embryos with the different genotypes were morphologically indistinguishable. They contained neuronal cells almost exclusively, as evaluated by phase-contrast and immunofluorescence microscopy using antibodies against Tau, Map2 and GFAP proteins (results not shown). $PS1^{+/+}$ and $PS1^{-/-}$ cultures were metabolically labelled and amyloid peptide and carboxy-terminal fragments from endogenously expressed mouse APP were analysed by immune precipitation (Fig. 1b, c). The strong inhibition of secretion of amyloid-β peptide and of the p3 fragment (generated by combined β- and γ-secretase and α- and γ-secretase proteolytic

activity[5], respectively; Fig. 1a), and the accumulation of C-terminal fragments of APP in $PS1^{-/-}$ neurons, demonstrates a direct role for PS1 in the amyloidogenic processing of mouse APP. Quantitative analysis of this effect was difficult because of the low signals obtained with endogenous mouse APP. We therefore expressed human wild-type APP and human APP containing the London (Val at position 642 to Ile) or Swedish (Lys at position 595 to Asn and Met 596 to Leu) clinical mutations in the neurons by using recombinant Semliki Forest virus (SFV)[9–12]. Using a panel of well characterized antibodies against APP the proteolytic processing of APP was analysed in $PS1^{-/-}$ cells (Fig. 1a). The catabolic intermediates visualized here have been previously identified by labelled-amino-acid sequencing[11]. Similar amounts of APP holoprotein (100K–140K) expression were obtained in $PS1^{+/+}$, $PS1^{+/-}$ and $PS1^{-/-}$ neuronal cultures (Fig. 1d). Secretion of APP ectodomain was the same in $PS1^{-/-}$ and in $PS1^{+/+}$ littermate controls (Fig. 1e), indicating that α- and β-secretase processing of APP was normal. This was confirmed using antibodies against amino-acid residues 595–612 (R1736; ref. 13) and residues 595–596 (ref. 14) of APP, which are specific for α- and β-secretase-cleaved APP ectodomain, respectively (Fig. 1f). Human amyloid-β peptide secretion detected by anti-APP597–612 (ref. 9) was significantly lower from the $PS1^{-/-}$ than from $PS1^{+/+}$ cells (Fig. 1g and Table 1). In control experiments using antibody 1282 (ref. 14), we confirmed the strong decrease in p3 secretion from virally transfected cells (results not shown), which was similar to that from uninfected cells (Fig. 1b). The fivefold decrease in amyloid peptide secretion was not accompanied by a concomitant accumulation of cell-associated amyloid peptide (Fig. 1h). In contrast, a twofold increase in β-secretase-cleaved and a fivefold increase in α-secretase-cleaved C-terminal fragments was observed in the cell extracts (Fig. 1d, h; Table 1).

In cultures derived from *PS1*-heterozygous embryos, either no or only weak effects on APP processing were observed (Fig. 1), in accordance with their normal phenotype[7,8]. APP containing either the London or the Swedish mutations that cause early-onset familial Alzheimer's disease (Fig. 1) underwent the same abnormal processing: a two- to fivefold accumulation of α- and β-secretase-cleaved C-terminal APP stubs in the cell extracts, a two- to fivefold inhibition of amyloid peptide secretion into the culture medium, and either no or only a marginal effect on secretion of APP ectodomain into the medium (Table 1).

The apparent paradox of an increase in C-terminal fragments in

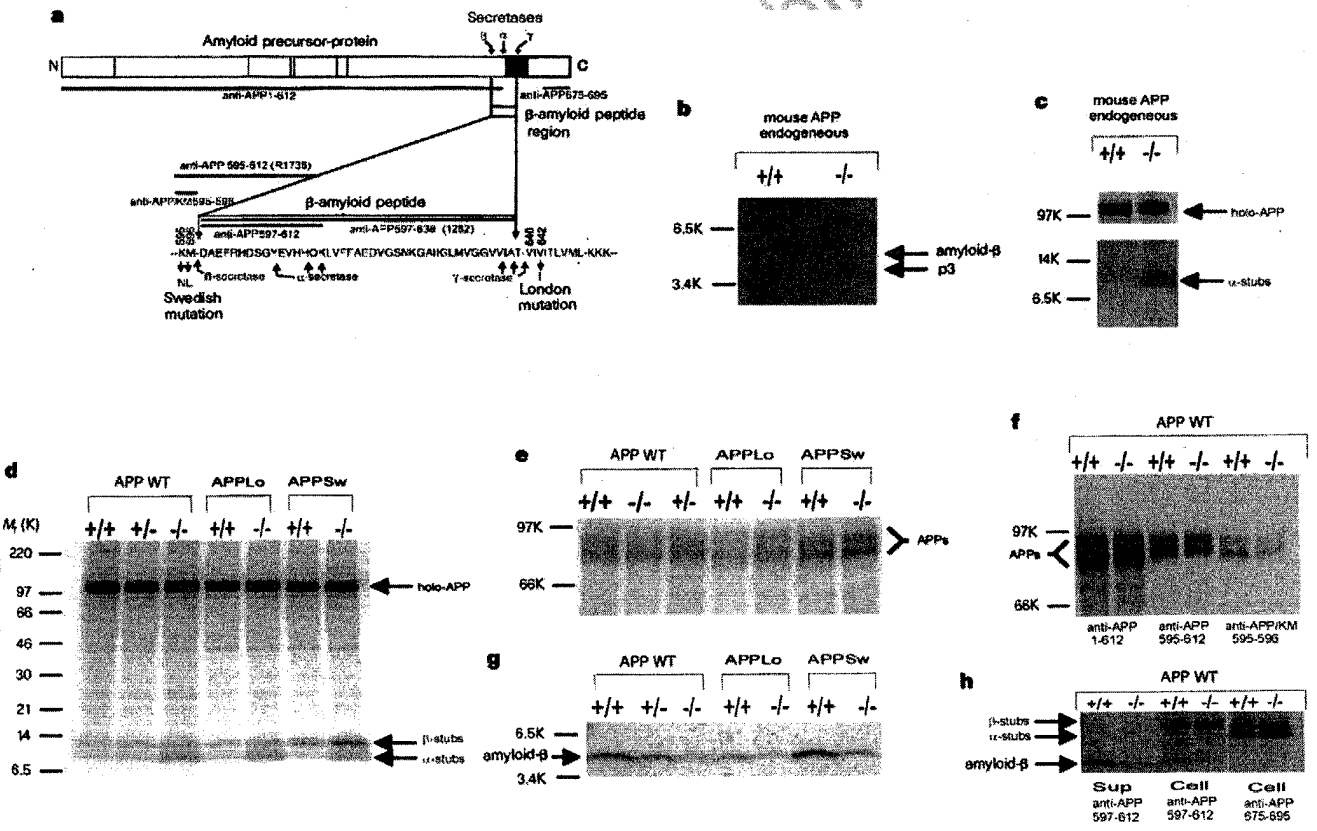

Figure 1 Processing of amyloid precursor protein. **a**, Structure of APP and the regions targeted by antibodies used in this study[9–14,29]. **b**, Amyloid-β and p3 peptide were immunoprecipitated from the medium of metabolically labelled neurons (for 18 h) with APP597–638 (R1282; ref. 13). **c**, Cell-associated APP (holo-APP) and C-terminal fragments were precipitated with APP675–695 (ref. 9) from cell extracts (normalized for TCA-precipitable label). Mainly α-secretase stubs are generated from mouse APP[9,11]. (See **a** for the cleavage sites[11].) **d**, Cell-associated APP fragments precipitated with anti-APP675–695 from neurons expressing human wild-type APP, or APP containing either the London (APP Lo) or the Swedish (APP Sw) mutation after infection with recombinant SFV[9–12]. For characterization of the β- and α-secretase-cleaved fragments, see ref. 11. **e**, Secreted APP ectodomain (APPs) was immunoprecipitated with anti-APP1–612 (ref. 29); the doublet appearance represents the different sialic acid content[11]. Note the small increase in mobility of APP Sw (APPsβ generated by β-secretase) compared to APPsα. **f**, Soluble APPs, APPsα and APPsβ precipitated with anti-APP1–612, anti-APP595–612 (R1736), and anti-APP595–596 (ref. 14), respectively. **g**, Secreted amyloid-β peptide precipitated with anti-APP597–612 (which does not react with p3)[9]. **h**, Amyloid-β peptide precipitated from medium ('Sup') and cell extracts ('Cell') using anti-APP597–612. β-Secretase-generated fragments (lanes 3, 4) coprecipitate with small amounts of cell-associated amyloid-β peptide. The intensity of the signals obtained for intracellular amyloid peptide is too low for reliable analysis (but see Fig. 3). Fragments generated by α- and β-secretase but no amyloid-β peptide are precipitated with anti-APP675–695, demonstrating the specificity of the signals in the previous two lanes.

cell extracts without a concomitant increase in APP ectodomain in the medium can be explained if PS1 is involved in γ-secretase processing of APP after cleavage by α- and β-secretase, resulting in turnover of these fragments. We verified this by pulse-chase experiments, which showed that newly generated C-terminal fragments of APP accumulated during four hours of chase in *PS1*$^{-/-}$ cells. In *PS1*$^{+/+}$ neurons, these fragments must be rapidly turned over as they were barely detectable at any time point (Fig. 2). The production of both amyloid-β(1–40) and amyloid-β(1–42) peptides in the medium of *PS1*$^{-/-}$ and wild-type neuronal cultures was measured by enzyme-linked immunosorbent assay (ELISA) and shown to be decreased 3.6- and 3.2-fold, respectively (Fig. 3). The two putative γ-secretases[15–17] appear to be equally affected by the *PS1* null mutation. We intend to investigate whether PS2 is responsible for the residual secretion of amyloid peptide in *PS1*$^{-/-}$ cultures by using *PS2*$^{-/-}$ mice and double-knockout embryos once they have been generated.

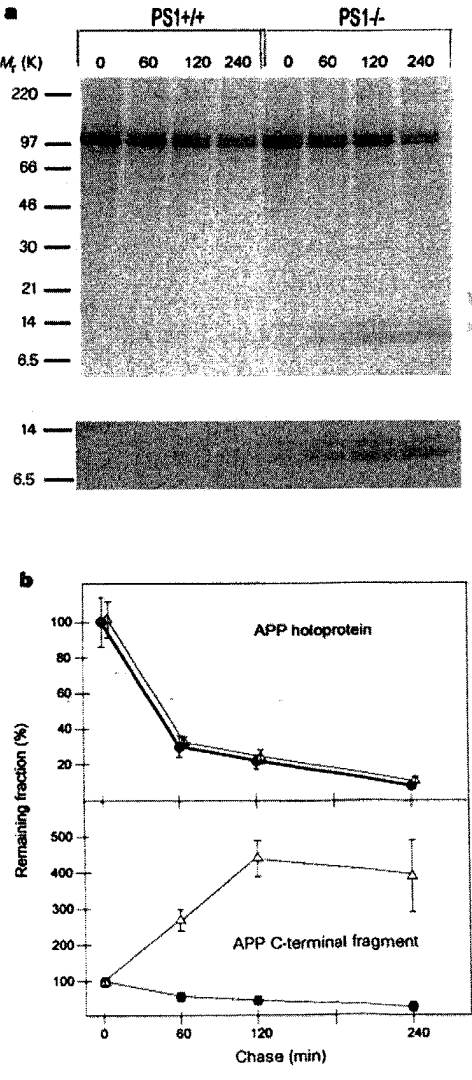

Figure 2 a, Pulse-chase experiment demonstrating similar turnover rates for APP holoprotein in PS1$^{+/+}$ and PS1$^{-/-}$ cultures. The lower half of the gel (after amplification of the signals) demonstrates the turnover of the C-terminal fragments. Pulse labelling, 30 min; chase, 60, 120 and 240 min. **b**, Quantitative analysis. All data are normalized[12] to the signal obtained at the end of the pulse labelling for APP holoprotein (top) and the carboxy-terminal fragments (bottom) from PS1$^{+/+}$ (●) and PS1$^{-/-}$ (△) cultures. Bars indicate s.e.m. ($n = 3$).

Table 1 Different APP fragments in *PS1*$^{-/-}$ and *PS1*$^{+/+}$ cultures

	APP WT	APP Lo	APP Sw
Cleaved stubs (β-secretase)	2.1 ± 0.4	2.3 ± 0.1	2.1 ± 0.3
Cleaved stubs (α-secretase)	5.4 ± 0.9	5.9 ± 1.6	4.6 ± 0.2
APP ectodomain (total)	1.0 ± 0.2	1.5 ± 0.1	0.9 ± 0.1
Amyloid-β peptide (total)	0.2 ± 0.1	0.4 ± 0.1	0.2 ± 0.0

All APP fragments (Fig. 1) were quantified by phosphorimaging in arbitrary densitometric volume units and normalized to the volume of APP holoprotein in the same culture to compensate for differences in cell numbers and infection[12]. The values obtained from *PS1*$^{-/-}$ cultures were divided by the values obtained in the *PS1*$^{+/+}$ cultures and this ratio is shown as the mean ± s.e.m. of three independent experiments. APP WT, wild-type APP; APP Lo, APP containing the London mutation (Val642→Ile); APP Sw, APP containing the Swedish mutations (Lys595→Asn and Met596→Leu).

Our results show that PS1 is involved in γ-secretase-mediated proteolytic cleavage of the C-terminal transmembrane fragments of APP after their generation by α- and β-secretase(s). PS1 is the only protein identified so far to be involved in one of the steps in APP processing by secretases. This mechanism may extend to other membrane-spanning proteins and suggests a physiological function for presenilin-1. Although PS1 itself may be (one of) the elusive γ-secretase(s), this is unlikely given the absence of sequence identity and lack of structural homology between PS1 and any proteinase domain known[1]. The residual amyloid-peptide secretion found for *PS1*$^{-/-}$ neurons suggests that PS1 is not the enzyme itself, but a regulatory cofactor in this processing step. The demonstration that APP and presenilins interact with one another fits this hypothesis[18,19]. The structural and functional similarity of PS1 and SCAP[6] may be significant: they both span the endoplasmic reticulum membrane 6 to 8 times[20–23] and both are involved in the cleavage of integral membrane proteins (APP and SREBP, respectively). PS1 and SCAP may represent a new class of chaperones that mediate or control access of proteinases to the transmembrane domain in the case of APP and to the lumenal-loop domain in the case of SREBP. An alternative explanation that PS1 is involved in the transport of the membrane-anchored C-terminal APP fragments towards the γ-secretase(s)-containing subcellular compartment does not necessarily contradict this hypothesis. Our data strongly support the idea that clinical mutations in *PS1* result in a gain of the function of PS1, and are not a haplotype insufficiency as was inferred from complementation experiments in *Caenorhabditis elegans* deficient in *sel12*, the worm's homologue of PS1 (refs 24,

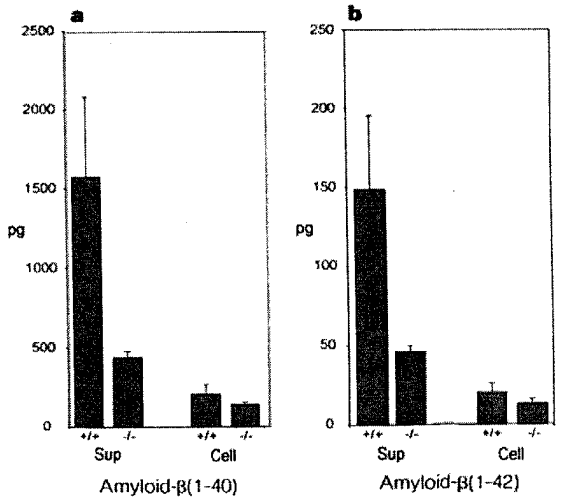

Figure 3 Assessment of the **a**, amyloid-β(1–40)-, and **b**, amyloid-β(1–42)-peptide contents in supernatants ('Sup') and cell extracts ('Cell') of PS1$^{+/+}$ and PS1$^{-/-}$ littermate neuronal cultures. The total amounts (in picograms) of peptide per culture dish are shown as mean ± s.d. ($n = 4$).

25). Our results indicate that production of amyloid peptide in neurons might be decreased by inhibiting PS1 function. With the proviso that PS1 function might be essential in adult brain, to be evaluated in conditionally targeted PS1 mice, PS1 may be a suitable target for anti-amyloidogenic therapy in Alzheimer's disease. □

Methods

Additional information describing the generation and characterization of the $PS1^{-/-}$ mice is available on our website http://www.med.kuleuven.ac.be/legtegg/.

The preparation of recombinant Semliki Forest virus stocks and the infection of neuronal cultures have been described[9–12]. Virus was diluted in culture medium and added to 3–5-day-old neuronal cultures. After viral adsorption (for 1 hour), the virus solution was replaced by normal medium. After 2 h, culture was continued in methionine-free medium containing 200 $\mu Ci\ ml^{-1}$ of [^{35}S]methionine. After 4 h of metabolic labelling, cell extracts and supernatants were processed as described[9–12]. Radioactive bands were measured as densitometric volumes using phosphorimaging. Immunoprecipitated material was resolved in 10–20% Tris–tricine gels or in 6% Tris–glycine gels for the analysis of APP fragments.

The sandwich-type ELISA[26,27] is based on capture antibodies 21F12 (specific for amyloid-β(1–42)) and FCA3340 (specific for amyloid-β(1–40))[28] and biotinylated reporter antibody 3D6. Synthetic peptides (Bachem) were used as standards. Controls showed no crossreactivity of the assay with shorter or longer forms of the peptides.

Received 15 September; accepted 20 November 1997.

1. Sherrington, R. *et al.* Cloning of a gene bearing missense mutations in early-onset familial Alzheimer's disease. *Nature* **375**, 754–760 (1995).
2. Scheuner, D. *et al.* Secreted amyloid β-protein similar to that in the senile plaques of Alzheimer's disease is increased *in vivo* by the presenilin 1 and 2 and APP mutations linked to Alzheimer's disease. *Nat. Med.* **2**, 864–870 (1996).
3. Hardy, J. Amyloid, the presenilins and Alzheimer's disease. *Trends Neurosci.* **20**, 154–159 (1997).
4. Haass, C. Presenilins: genes for life and death. *Neuron* **18**, 687–690 (1997).
5. Haass, C. & Selkoe, D. J. Cellular processing of β-amyloid precursor protein and the genesis of amyloid β-peptide. *Cell* **75**, 1039–1042 (1993).
6. Brown, M. S. & Goldstein, J. L. The SREBP pathway: regulation of cholesterol metabolism by proteolysis of a membrane-bound transcription factor. *Cell* **89**, 331–340 (1997).
7. Wong, P. C. *et al.* Presenilin 1 is required for Notch-1 and Dll1 expression in the paraxial mesoderm. *Nature* **387**, 288–292 (1997).
8. Shen, J. *et al.* Skeletal and CNS defects in presenilin-1 deficient mice. *Cell* **89**, 629–639 (1997).
9. De Strooper, B. *et al.* Production of intracellular amyloid-containing fragments in hippocampal neurons expressing human amyloid precursor protein and protection against amyloidogenesis by subtle amino acid substitutions in the rodent sequence. *EMBO J.* **14**, 4932–4938 (1995).
10. Tienari, P. *et al.* Intracellular and secreted Alzheimer β-amyloid species are generated by distinct mechanisms in cultured hippocampal neurons. *Proc. Natl Acad. Sci. USA* **94**, 4125–4130 (1997).
11. Simons, M. *et al.* Amyloidogenic processing of the human amyloid precursor protein in primary cultures of rat hippocampal neurons. *J. Neurosci.* **16**, 899–908 (1996).
12. Saftig, P. *et al.* Amyloidogenic processing of human amyloid precursor protein in hippocampal neurons devoid of cathepsin D. *J. Biol. Chem.* **44**, 27241–27244 (1996).
13. Haass, C. *et al.* Amyloid β-peptide is produced by cultured cells during normal metabolism. *Nature* **359**, 322–325 (1992).
14. Chyung, A. S. C. *et al.* Novel β-secretase cleavage of amyloid precursor protein in the endoplasmic reticulum/intermediate compartment of NT2N cells. *J. Cell Biol.* **138**, 671–680 (1997).
15. Citron, M. *et al.* Evidence that the 42- and 40-amino acid forms of amyloid β protein are generated from the β-amyloid precursor protein by different protease activities. *Proc. Natl Acad. Sci. USA* **93**, 13170–13175 (1996).
16. Klafki, H. W. *et al.* The carboxy-terminal termini of β-amyloid peptides 1–40 and 1–42 are generated by distinct γ-secretase activities. *J. Biol. Chem.* **45**, 28655–28659 (1996).
17. Hartmann, T. *et al.* Distinct sites of intracellular production for Alzheimer's disease $A\beta_{40/42}$-amyloid peptides. *Nature Med.* **3**, 1016–1020 (1997).
18. Weidemann, A. *et al.* Formation of stable complexes between two Alzheimer's disease gene products: presenilin 2 and β-amyloid precursor protein. *Nature Med.* **3**, 328–332 (1997).
19. Xia, W. *et al.* Interaction between amyloid precursor protein and presenilins in mammalian cells: implications for the pathogenesis of Alzheimer's disease. *Proc. Natl Acad. Sci. USA* **94**, 8208–8213 (1997).
20. Doan, A. *et al.* Protein topology of presenilin 1. *Neuron* **17**, 1023–1030 (1996).
21. Li, X. & Greenwald, I. Membrane topology of the *C. elegans* SEL-12 presenilin. *Neuron* **17**, 1017–1021 (1996).
22. Lehmann, S., Chiesa, R. & Harris, D. A. Evidence for a six-transmembrane domain structure of presenilin-1. *J. Biol. Chem.* **272**, 12047–12051 (1997).
23. De Strooper, B. *et al.* Phosphorylation, subcellular localization, and membrane orientation of the Alzheimer's disease-associated presenilins. *J. Biol. Chem.* **272**, 3590–3598 (1997).
24. Levitan, D. *et al.* Assessment of normal and mutant human presenilin function in *Caenorhabditis elegans*. *Proc. Natl Acad. Sci. USA* **93**, 14940–14944 (1996).
25. Baumeister, R. *et al.* Human presenilin-1, but not familial Alzheimer's disease (FAD) mutants, facilitate *Caenorrhabditis elegans* Notch signalling independently of proteolytic processing. *Genes Funct.* **1**, 149–159 (1997).
26. Citron, M. *et al.* Mutant presenilins of Alzheimer's disease increase production of 42-residue amyloid β-protein in both transfected cells and transgenic mice. *Nature Med.* **3**, 67–72 (1997).
27. Vanderstichele, H. *et al.* in *Progress in Alzheimer's and Parkinson's Diseases* (eds Fisher, A., Yoshida, M. & Hanin, I.) (Plenum, New York, in the press).
28. Barelli, H. Characterization of new polyclonal antibodies specific for 40- and 42-amino-acids-long amyloid β peptides: their use to examine the cell biology of presenilins and the immunohistochemistry of sporadic Alzheimer's disease and cerebral amyloid angiopathy cases. *Mol. Med.* **3**, 695–707 (1997).
29. De Strooper, B. *et al.* Basolateral secretion of amyloid precursor protein in MDCK cells is disturbed by alterations of intracellular pH and by introducing a mutation associated with familial Alzheimer's disease. *J. Biol. Chem.* **270**, 4058–4065 (1995).

Acknowledgements. This work was supported by the FWO-Vlaanderen, the Flemish Action Program for Biotechnology (VLAB), the Flemish Institute for Biotechnology (VIB), the K.U.Leuven, the Human Frontier of Science Program (HFSP), the Deutsche Forschungsgemeinschaft and the Fonds der Chemischen Industrie. We thank B. Greenberg for antibodies anti-APP1-612 and anti-APPKM595/596, D. Selkoe for R1736 and R1282, and F. Checler for FCA3340, C. Dotti, B. Nelissen and E. Vanmechelen for advice; and S. Tiereliers for technical assistance.

Correspondence and requests for materials should be addressed to B.D.S. (cell biology) or P. Saftig (transgenic mice) (e-mail addresses: Bart.Destrooper@med.kuleuven.ac.be and Saftig@uni-bc2.gwdg.de).

NIP domain prevents N-type inactivation in voltage-gated potassium channels

Jochen Roeper*‡, Sabine Sewing*‡, Ying Zhang*, Tobias Sommer*, Siegmund G. Wanner† & Olaf Pongs*

** Zentrum für Molekulare Neurobiologie Hamburg, Institut für Neurale Signalverarbeitung, Martinistrasse 52, D-20246 Hamburg, Germany*
† Institut für Biochemische Pharmakologie, Unviersität Innsbruck, Medizinische Fakultät, Peter-Mayrstrasse 1, A-6020 Innsbruck, Austria
‡ These authors contributed equally to this work.

***Shaker*-related voltage-gated K^+ (K_v) channels[1,2] are assembled from ion-conducting $K_v\alpha$ subunits, which are integral membrane proteins, and auxiliary $K_v\beta$ subunits. This leads to the formation of highly diverse heteromultimeric K_v channels that mediate outward currents with a wide range of time courses for inactivation. Two principal inactivation mechanisms have been recognized[1]: C-type inactivation correlated with carboxy-terminal $K_v\alpha$-subunit structures[3], and N-type inactivation conferred by 'ball' domains in the amino termini of certain $K_v\alpha$[4,5] and $K_v\beta$[6] subunits. Assembly of heteromultimers with one or more $K_v\alpha$[4,7]- and/or $K_v\beta$[6] ball domains appears to be an essential principle of the generation of A-type K_v channel diversity. Here we show that, unexpectedly, the presence of $K_v\alpha$- or $K_v\beta$-ball domains does not dominate the gating phenotype in heteromultimers containing $K_v1.6\alpha$ subunits. These heteromultimers mediate non-inactivating currents because of the dominant-negative activity of a new type of N-type inactivation-prevention (NIP) domain present in the $K_v1.6$ amino terminus. Mutations in the NIP domain lead to loss of function, and its transfer to another $K_v\alpha$ subunit leads to gain of function. Our discovery of the NIP domain, which neutralizes the activity of $K_v\alpha$- and $K_v\beta$-inactivation gates, establishes a new determinant for the gating behaviour of heteromultimeric K_v channels.**

Unlike in other $K_v1\alpha/K_v\beta1.1$ heteromultimers[6,8], such as $K_v1.5/K_v\beta1.1$ ($\tau_h = 1.5 \pm 0.2$ ms, $n = 6$; Fig. 1a), $K_v\beta1.1$ did not confer rapid N-type inactivation to non-inactivating $K_v1.6$ channels ($n = 5$; Fig. 1b). Coexpression of $K_v\beta1.1$ with $K_v1.6$, however, shifted the voltage-dependent activation of the $K_v1.6$ outward currents ($V_{1/2} = 15 \pm 2.7$ mV, slope factor 12 ± 1.1 mV, $n = 4$) to more negative potentials ($V_{1/2} = 4.9 \pm 4.9$ mV, slope factor 8.9 ± 1.2 mV, $n = 5$). Similar shifts in the voltage dependence of activation had been observed with $K_v\beta2$ subunits, which do not possess a ball domain, when coexpressed with $K_v1\alpha$ subunits[8,9]. Thus $K_v\beta1.1$ apparently influenced $K_v1.6$ channel gating like a $K_v\beta$ subunit without an inactivation gate. This implies that $K_v1.6/K_v\beta1.1$ heteromultimers were formed, as suggested by co-immunoprecipitation studies[10]. The $K_v1.6$ N terminus contains a conserved functional $K_v\beta1$-binding site[11,12], as indicated by protein overlay binding